II-VI oxides phase separate whereas the corresponding carbonates order: The stabilizing role of anionic groups

J. A. Chan and Alex Zunger*

National Renewable Energy Laboratory, Golden, Colorado 80401, USA

(Received 24 August 2009; published 6 October 2009)

The formation enthalpies of isovalent, isostructural rocksalt alloys, (A,B), where $X=O$ such as $(Ca,Mg)O$, are typically unfavorable (positive) for both ordered and random phases. Simple replacement of the single-atom anion, X, by a larger anionic group, such as CO_3 or SO_4, is able to induce a favorable (negative) formation enthalpy, leading to the formation of the ordered alternate monolayer, $(CaCO_3)_1/(MgCO_3)_1$, dolomite structure. The underlying cause of this behavior is analyzed by breaking down the formation process in a Born-Haber-*like* cycle into volume and cell-shape deformation, chemical exchange, and cell-internal relaxation using *first-principles* density-functional theory calculations in the generalized gradient approximation. It is found that when the anion is a group (CO_3), rather than a single atom (O), the energy gained from the internal relaxation overcomes the energy required to compensate the volume mismatch. This explains the general experimental trends of phase separation in isovalent, isostructural alloys without internal-anion structure, compared to ordering tendencies when the anionic group removes internal strain. The importance of obtaining structural ideality in the design of stable solid solutions is highlighted.

PACS number(s): 61.66.Dk, 61.50.Ah, 61.43.Dq

I. INTRODUCTION

Alloying of binary AX and BX constituents is commonly used in electronic and optoelectronic technology to achieve material properties (such as band gap, effective masses, or lattice parameters) not available from the rather limited repertoire of the base (individual AX and BX) octet compounds IV-IV, III-V, or II-VI. To be useful, such $A_xB_{1-x}X$ alloys are required to be spatially homogeneous, for precipitates or clusters often impede carrier transport. At low temperatures, all $A_xB_{1-x}X$ alloys either phase separate inhomogeneously into their constituents or order crystallographically into a single homogeneous phase, the distinction depending on the sign of the formation enthalpy,

$$\Delta H(x) = E(A_xB_{1-x}X) - [xE(AX) + (1-x)E(BX)] \quad (1)$$

where E represents the total internal energy. Alloys with *positive formation enthalpy* will hence phase separate at low temperatures and become usefully homogeneous only above the miscibility temperature, $T_{MG}(x)$, where the excess free energy $\Delta H - T_{MG}\Delta S$ becomes negative on account of the random-alloy entropic $-T_{MG}\Delta S$ term overcoming the $+\Delta H$. Alloys with *negative formation enthalpy* will order crystallographically at low temperature and disorder above the order-disorder transition temperature, T_C. It turns out that virtually all isovalent and isostructural octet alloys used in optoelectronics[1–5] have $\Delta H > 0$. This includes the IV-IV group, Si-Ge, Ge-Sn, and Si-Sn (except Si-C),[6] the III-V group such as GaAs-InAs or GaN-InN (except AlInX_2, $X=$P, or As, in the chalcopyrite structure[7]) and the II-VI group including group II$_B$ metals ZnS-ZnSe, CdTe-HgTe, or group I$_A$ oxides CaO-MgO, BaO-CaO (except NiO-MgO) (Ref. 8) as well as alkali halides[2] (except LiF-CsF and related materials[9,10]).

Interestingly, nature offers a special category of $\Delta H < 0$ systems among isovalent and isostructural octet $A_xB_{1-x}X$ alloys: when X is a single-atom anion, then generally $\Delta H > 0$,

and phase separation becomes inevitable as demonstrated above, but when X is an anionic *group* such as the carbonate, $X=CO_3$, or sulfate, $X=SO_4$, it often happens that $\Delta H < 0$ and long-range alloy ordering ensues.[8,11] This is illustrated for $X=O$ vs $X=CO_3$ in the first three columns of Table I, where first-principles calculated as well as measured formation enthalpies are given for both ordered [an example is shown in Fig. 1(a)] and random (see footnote[12]) phases of CaO-MgO equimolar alloys, demonstrating $\Delta H > 300$ meV/cation pair for both phases whereas for CaCO$_3$-MgCO$_3$ equimolar alloys $\Delta H \sim -40$ meV/cation pair in the ordered (dolomite) phase and $\sim +150$ meV/cation pair in the random equimolar alloy. Indeed, the CaO-MgO alloy easily phase separates below $T \sim 2000\,^{\circ}$C[13] whereas CaCO$_3$-MgCO$_3$ orders crystallographically into the (111) alternate monolayer dolomite structure [Fig. 1(b)] on account of its $\Delta H < 0$ in the ordered phase.[14–17] Similar cases where solubility is enhanced (ΔH becomes less positive) are when the single-anion X is replaced by the anionic *group* in *isovalent* and *isostructural* alloys including $(Ca,Mg)SO_4$ (Refs. 11 and 18) and $(Ba,Ca)_2SiO_4$.[19] The increased solubility of carbonates or sulfates has been taken advantage of by experimentalists to synthesize the high-concentration oxides by the use of thermodecomposition of ACO_3-BCO_3 to get AO-BO, e.g., (Ca,Mg),[11] (B,Sr),[20] even triple carbonate systems such as (Ba,Sr,Ca).[21]

Although none of these systems is particularly useful in optoelectronics, we wish here to discover the underlying mechanism that enables such a significant reduction of the natural tendencies for volume-mismatched cations to unmix when the anion changes into an anionic *group*. For this reason, we focus on the *isovalent* CaO-MgO and CaCO$_3$-MgCO$_3$ systems since, for *nonisovalent* systems, for example, where one of the metal cation species has active d orbitals, strong chemical interactions are likely to become important and can mask the ΔH-lowering effects due to the internal degrees of freedom of the common anion group.

TABLE I. Formation enthalpies, ΔH, and breakdown of the formation enthalpies into ΔE_{VD} (volume deformation), ΔE_{SD} (shape deformation), ΔE_{CE} (chemical exchange), and ΔE_{SR} (structural relaxation) [meV/cation pair] for the CaO-MgO and $CaCO_3$-$MgCO_3$ systems.

System	Phase	ΔH	ΔH Literature	ΔE_{VD}	ΔE_{SD}	ΔE_{CE}	ΔE_{SR}
CaO-MgO	Ordered (001)	618	564[a]	659	0	−40	−1
	Ordered (111)	337	376[a]	676	0	−112	−227
	Random	394	327[b]	665	0	−72	−199
$CaCO_3$-$MgCO_3$	Ordered (111)	−39	−76[c], −83[d], −96[e]	608	251	−11	−886
	Random	147	124[c],124–165[d],247[e]	598	222	−5	−669

[a]Calculated, Ref. 23 with Kleinman-Bylander pseudopotentional local-density approximation (LDA).

[b]Calculated, Ref. 31, with ultrasoft pseudopotentional LDA.

[c]Calculated, Ref. 39, with Vanderbilt pseudopotential DFT (ordered) and first-principles phase-diagram calculations (random).

[d]Calculated, Ref. 41, with interatomic potential calculations.

[e]Experiment, Ref. 17.

Solid solutions CaO-MgO and $CaCO_3$-$MgCO_3$ are often used as prototype systems for the basis of theoretical studies, and there are numerous previous calculations that have investigated the energies of point defects [CaO-MgO (Refs. 22–24) and $CaCO_3$-$MgCO_3$ (Refs. 25 and 26)], surfaces [for example, Refs. 27 and 28)], and the solid solutions in the bulk phase [CaO-MgO (Refs. 22, 23, and 29–35) and $CaCO_3$-$MgCO_3$ (Refs. 36–41)]. These have shown that minimizing volume mismatch and maximizing internal relaxation are the most important effects for lowering ΔH in these systems. Since ΔH of Eq. (1) often scales with the volume-mismatch (V_{AX}-V_{BX}) between constituents packed into the lattice,[1,4,8,33] the reduced ΔH of the carbonate system with respect to the oxide system is thought to be due to its smaller relative volume mismatch (32%) compared to the corresponding oxide[8,11] (with 47% mismatch). However, as will

FIG. 1. (Color online) (a) Rocksalt alloy with CaO-MgO layering in the (111) conventional cell direction, (b) Ordered dolomite, with $CaCO_3$-$MgCO_3$ layering in the (111) direction of the conventional cell of the distorted rocksalt-type lattice. The atoms are calcium (blue/gray spheres), magnesium (red/dark gray spheres), oxygen (small gray spheres), and carbon (small green/gray spheres), where the triangles highlight the planar carbonate groups. The orange hexagons highlight the parts of the structure shown in Fig. 3.

be shown below, the energy ΔE_{VD} required to deform the constituents, from their natural unit-cell size to the volume they occupy in the 50–50 % alloy is ∼600 meV/cation pair for $CaCO_3$-$MgCO_3$, and ∼650 meV/cation pair, for CaO-MgO (viz., "ΔE_{VD}" in Table I). Significantly, the values in both systems are very large and positive and do not disclose how the total ΔH of the ordered carbonate becomes negative. In this work, the behavior is analyzed by breaking down the formation process, a method previously applied by Refs. 7, 31, and 42–44, for select ordered superlattice and random structures of CaO-MgO and $CaCO_3$-$MgCO_3$. The structural and energetic changes are then examined at each of the steps, including: volume and cell-shape deformation of the constituents, ΔE_{VD}, and ΔE_{SD}, chemical exchange ΔE_{CE}, attendant upon bringing together the "prepared" constituents to form the mixed phase without changing its volume, and cell-internal atomic relaxation, ΔE_{SR}, attendant upon letting the atoms in the mixed phase relax to their energy-lowering positions. We find that (i) as previously noted, the unfavorable mixing of oxide solid solutions is due to volume mismatch, evident from the large volume deformation energy ΔE_{VD} that outweighs all other terms. However, the favorable mixing for ordered dolomite is not due to reduced volume mismatch as previously suggested since the volume deformation is now accompanied by an energetically costly cell-shape deformation, (ii) the favorable mixing for ordered dolomite is due to relaxation of the strong C-O bonds in the CO_3 group, which permit the M-O bonds to come closer to ideality compared to the oxides, and (iii) the formation of the *random* carbonate is unfavorable due to disruption of the CO_3 bond lengths and angles from ideal values. Achieving structural ideality for the strongest bonds in the structure is the most important factor for obtaining a favorable enthalpy.
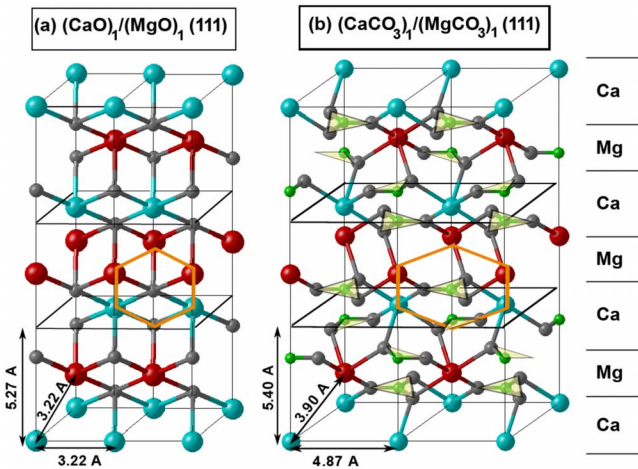
Conceptual breakdown of the formation enthalpy into physical contributions

CaO and MgO occur in the cubic rocksalt structure and random CaO-MgO alloys are formed by randomly occupying the metal sublattice of rocksalt by Ca and Mg. The hypothetical ordered $(CaO)_1/(MgO)_1$ structure with layering
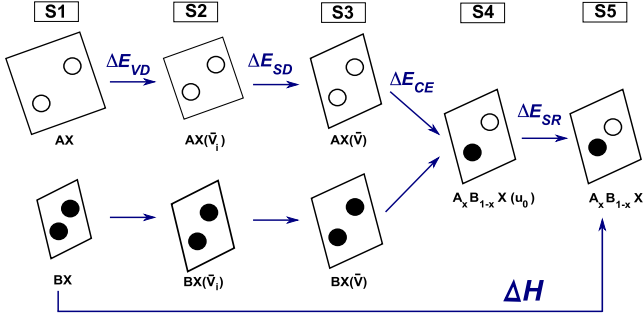
FIG. 2. (Color online) Schematic showing the formation enthalpy, ΔH, of $A_x B_{1-x} X$ (S5) with respect to its constituent binaries, AX and BX (S1), and the corresponding breakdown of ΔH into physical steps for analysis via: volume deformation, ΔE_{VD}, cellshape deformation, ΔE_{SD}, chemical exchange, ΔE_{CE} and structural relaxation, ΔE_{SR}.

along the (111) direction of the rocksalt conventional cell is shown in Fig. 1(a). Calcite, $CaCO_3$, (and magnesite, $MgCO_3$), (space group $R\bar{3}c$) has a structure analogous to rocksalt, where the Ca (Mg) and C atoms make up a (distorted) rocksalt lattice and the C-O bonds in the planar CO_3^{2-} group are along the planes in the (111) direction of the rocksalt conventional cell. The (111) layered structure of dolomite, $(CaCO_3)_1/(MgCO_3)_1$, (space group $R\bar{3}$) consists of alternating pure Ca, and pure Mg layers along the (111) planes, separated by CO_3 layers [Fig. 1(b)].

The method of analysis is performed in two parts: first, the formation enthalpy, $\Delta H(x)$ from Eq. (1) are calculated for the ordered and random structures of CaO-MgO and $CaCO_3$-$MgCO_3$ (Sec. III). Second, each value of $\Delta H(x)$ is broken down into separate, physical steps for analysis in a Born-Haber-*like* cycle[22,43] (Secs. IV–VI). Each step is described diagrammatically in Fig. 2 and mathematically as follows:

(1) Volume deformation, ΔE_{VD}, is the energy required to isotropically deform both pure AX with equilibrium V_{AX} and BX with equilibrium V_{BX} (structure S1) to the volume, $\bar{V}$, that AX and BX occupy in the final, fully relaxed AX-BX structure, (structure S2) (where I highlights the isotropic deformation).

$$\Delta E_{VD}(x) = \Delta E_{(S2-S1)} = x[E_{AX}(\bar{V}_I) - E_{AX}(V_{AX})] + (1-x)$$
$$\times [E_{BX}(\bar{V}_I) - E_{BX}(V_{BX})] \quad (2)$$

(2) Cell-shape deformation, ΔE_{SD}, is the energy required for the cell-shape (i.e., ratio between lattice parameters a:b:c) of the S2 structures, to deform to that of the final mixed-phase structure, keeping the volume fixed. This results in structures $AX(\bar{V})$ and $BX(\bar{V})$ (called S3),

$$\Delta E_{SD}(x) = \Delta E_{(S3-S2)}$$
$$= x[E_{AX}(\bar{V}) - E_{AX}(\bar{V}_I)] + (1-x)[E_{BX}(\bar{V}) - E_{BX}(\bar{V}_I)]$$
$$(3)$$

ΔE_{SD} is negligible when the a:b:c ratios are the same for

AX, BX, and AX-BX structures. An example is the CaO-MgO (001) system where cubic symmetry is retained such that $a=b=c$.

(3) Chemical exchange, ΔE_{CE}, is the energy to bring together AX and BX, already prepared at $\bar{V}$ and the final equilibrium cell shape, into the structure of the ordered AX/BX or the random $A_x B_{1-x} X$ alloy, without internal relaxation,

$$\Delta E_{CE}(x) = \Delta E_{(S4-S3)}$$
$$= E_{(A_x B_{1-x} X)}(\bar{V}; u_0) - [xE_{AX}(\bar{V}) + (1-x)E_{BX}(\bar{V})]$$
$$(4)$$

Where u_0 denotes the unrelaxed cell-internal ionic positions (consistent with the space-group symmetry of AX and BX).

(4) Structural relaxation, ΔE_{SR}, is the energy gained by the relaxation of the cell-internal ionic positions to the final relaxed structure.

$$\Delta E_{SR}(x) = \Delta E_{(S5-S4)} = E_{(A_x B_{1-x} X)}(\bar{V}) - E_{(A_x B_{1-x} X)}(\bar{V}; u_0)$$
$$(5)$$

These four components sum up to give the formation enthalpy [Eq. (1)]

$$\Delta H(x) = \Delta E_{(S5-S1)}$$
$$= \Delta E_{VD} + \Delta E_{SD} + \Delta E_{CE} + \Delta E_{SR}$$
$$= E_{(A_x B_{1-x} X)}(\bar{V}) - [xE_{AX}(V_{AX}) + (1-x)E_{BX}(V_{BX})]$$
$$(6)$$

II. COMPUTATIONAL METHODOLOGY

The calculations are performed using *first-principles* density-functional theory (DFT) in the Perdew-Burke-Ernzerhof generalized gradient approximation using the standard projector-augmented wave (PAW) pseudopotentials with valence electron configurations of $Ca: 3s^2 3p^6 4s^2$, $Mg: 2p^6 3s^2$, $C: 2s^2 2p^2$, and $O: 2s^2 2p^4$ (Ref. 45). The energy cutoff for the plane-wave expansion is 400 eV and gammacentered k-point sampling is used to converge total energies to better than 0.5 meV/cation (see footnote[46]). The mixed ordered or random structures studied here are all with the $x_{Mg}=50\%$ composition. We model completely random phases (i.e., with no short or long-range ordering) using special quasirandom structures (SQS) which mimic the completely random alloy.[47] The occupation of the lattice sites by Ca or Mg atoms is done in a controlled way so as to best mimic the atom-atom correlation functions of the corresponding infinite random arrangement. The SQS structure used to simulate the random oxide consists of a 16-cation (32-atom) cell and mimics the random alloy up to the seventh nearest-neighbor pair, the seventh triplet and the second quadruplet. The volume is relaxed under the constraint that $a=b=c$. For the random carbonate, the SQS structure consists of a 16-cation (80-atom) cell, and mimics the random alloy up to the sixth nearest-neighbor pair and the fourth triplet. The volume is relaxed under the constraint that a

TABLE II. Calculated lattice parameters, a (Å) and c/a ratios of the conventional cells of the CaO, MgO, CaCO$_3$, MgCO$_3$, and their mixed phases compared with experiment.

System	Phase	a (Å)	Expt.	c/a	Expt.
CaO-MgO	CaO	4.840	4.803[a]	1	1[a]
	MgO	4.258	4.207[a], 4.211[b]	1	1[a]
	Ordered (001)	4.606		1	
	Ordered (111)	4.559		1	
	Random	4.579		1	
CaCO$_3$-MgCO$_3$	CaCO$_3$	5.053	4.989[c]	3.414	3.416[c]
	MgCO$_3$	4.692	4.636[c]	3.241	3.240[c]
	Ordered (111)	4.865	4.807[d],4.803[e]	3.327	3.329[d],3.328[e]
	Random	4.874	4.804[d]	3.328	3.346[d]

[a]Reference 48.
[b]Reference 49.
[c]Reference 50.
[d]Reference 16. No long-range order detected in x-ray diffraction but may have considerable short-range order (Ref. 17).
[e]Reference 14.

$=b \neq c$, where c/a is constrained to that obtained by a linear relation from the calculated geometry-relaxed CaCO$_3$ and MgCO$_3$. The $a:b:c$ ratios are constrained for the SQS structures in order to preserve the symmetry of the random alloy at the thermodynamic limit. Note the values of a, b, and c are all fully relaxed within this constraint.

III. FORMATION ENTHALPIES OF RANDOM AND ORDERED CaO-MgO AND CaCO$_3$-MgCO$_3$

Table II confirms that the current method reproduces the experimental lattice parameters well for single oxides and carbonates, as well as for the mixed carbonates. The c/a ratios are very close to those in experiment showing the structural features are accurately modeled, this is particularly important for the cell-shape deformation step, ΔE_{SD} of Eq. (3).

The formation enthalpies are summarized in Table I. The CaO-MgO ΔH are comparable to previous DFT calculations[23,31] and are positive for both ordered and random structures. The authors are not aware of experimental values for comparison but the positive ΔHs are in agreement with the experimental phase diagram where solid phase separation into the pure binaries occurs from 2370 °C down to the lowest measured temperature (1600 °C).[13]

For CaCO$_3$-MgCO$_3$, the observed negative ΔH for the ordered dolomite $[(CaCO_3)_1/(MgCO_3)_1(111)]$ and positive ΔH of the random $(CaCO_3)_{0.5}(MgCO_3)_{0.5}$ phase[16,17] is reproduced by the calculations. Dolomite is calculated to have a formation enthalpy of -39 meV/cation pair using PAW pseudopotentials. This value differs from previous calculations[39] (Table I), which, however, employ the more approximate Vanderbilt-type pseudopotentials. The calculated formation enthalpy of the random alloy is $+147$ meV/cation pair, which is in good agreement with pre-

vious predictions[39,41] but significantly smaller in magnitude compared to experiment.[17] The reason why the experimental value is larger may be due to the existence of domains in the experimental samples. The CO$_3$ groups in the random alloy relaxes in the same *general* direction as for the ordered dolomite [Fig. 1(b)], facing in the same general direction on each plane, then opposite direction on the next. Thus the calculations do not include the presence of domains, for example, where CO$_3$ in one plane align along one direction, but, on crossing the domain boundary now align along the opposite direction. The presence of such domains have been observed in synthetically produced samples[51] and can raise the ΔH value compared to the theoretical prediction.

In order to explain the origin of the formation enthalpies, we now turn to the breakdown of the formation enthalpy into components as described by Eqs. (2)–(5).

IV. THE VOLUME AND CELL-SHAPE DEFORMATION: ΔE_{VD} AND ΔE_{SD}

The fifth column of Table I shows the energy, ΔE_{VD}, to deform the constituent CaO and MgO (overcoming the 47% volume mismatch of the single oxides, Table II) to the common volume of the final CaO-MgO structure, to be at least 650 meV/cation pair. The hypothetical ordered $(CaO)_1/(MgO)_1$ (111) layered structure undergoes a slight rhombohedral distortion, (the lattice angle distorts from cubic, $\alpha=90.0°$, to $\alpha=86.4°$) whereas the cell shape is constrained by symmetry for the ordered (001), and fixed for the random structure in order to mimic the random phase at the thermodynamic limit. In all cases ΔE_{SD} is negligible (<1 meV/cation pair). The large value of ΔE_{VD} (summed with ΔE_{SD}) means volume mismatch is the most significant contribution to ΔH for random and ordered oxides. This is in agreement with many studies that hold the view that the

positive ΔH of oxides is due to the strain induced by large volume mismatch (47%) between the initial binaries (for example, Refs. 8, 24, 31, 33, and 34). For the carbonates ΔE_{VD} values are somewhat smaller than for the oxides, ~600 meV/cation pair (Table I), as expected by the smaller (32%) volume mismatch between the single carbonates (Table II). However, the extra energy required to deform the lattice angles, $\Delta E_{SD} = 200$ meV/cation pair brings the total energies required to deform the single carbonates to the final volume and shape of the ordered dolomite and random structures to 858 and 821 meV/cation pair, respectively. This shows that the lowered formation enthalpy of the ordered carbonate is not entirely due to reduced volume mismatch as previously suggested[8,11] since this is accompanied by energetically costly lattice shape deformation.

V. DECORATION OF METAL SUBLATTICE BY DIFFERENT CATIONS AT FIXED VOLUME: ΔE_{CE}

Tepesch *et al.*[22] theorizes that the chemical exchange energy, ΔE_{CE}, for CaO-MgO should be negligible because Ca and Mg are isovalent. The present calculations find that ΔE_{CE}, is in fact quite significant, particularly for the ordered (111) and random oxide structures (Table I). Previous observations have shown that when charge transfer occurs, often from larger cation to the smaller cation[43] in the direction of increased electronegativity, then $\Delta E_{CE} < 0$, but when charge transfer opposes the preferred direction due to electronegativity, $\Delta E_{CE} > 0$.[7] This is seen for the ordered (111) oxide, there is a decrease in atomic charge from the valence orbitals on Ca ($\Delta e = -0.09e$) in the mixed phase compared to the CaO binary, in conjunction with an increase in atomic charge on Mg ($\Delta e = \sim 0.03e$) compared to the MgO binary (see footnote[52]). For the ordered (111) carbonate the charge differences are $\Delta e = -0.12e$ on Ca and $\Delta e = 0.06e$ on Mg, giving small but clearly negative ΔE_{CE} (Table I). The interaction is reduced with distance in both oxides and carbonates since ΔE_{CE} (Table I) becomes smaller in magnitude with the increase in lattice parameter, a (Table II).

VI. CELL-INTERNAL RELAXATION: ΔE_{SR}

A. Oxides

The energy gained on relaxation of the internal coordinates, ΔE_{SR}, for the (111) ordered and random structure are substantial (−200 meV/cation pair) while almost negligible for the (001) ordered structure. For the (111) ordered and random structures, the Ca-O distance increases and the Mg-O distance decreases in an asymmetric relaxation centered on the oxygen [shown for the ordered (111) structure in Fig. 3(a)] to become closer to ideal bond lengths (see footnote[53]) as shown by the change from S4 to S5 in Table III. The symmetry of the (001) ordered structure forces Ca-O and Mg-O bond lengths to be equal so there is little change between S4 and S5 structures (Table III). The bond lengths of the random phase can relax (Note: the bond lengths shown for the random phase are averaged values and can only give an *indication* of the bond lengths) but due to the random cation arrangement does not gain as much energy from the
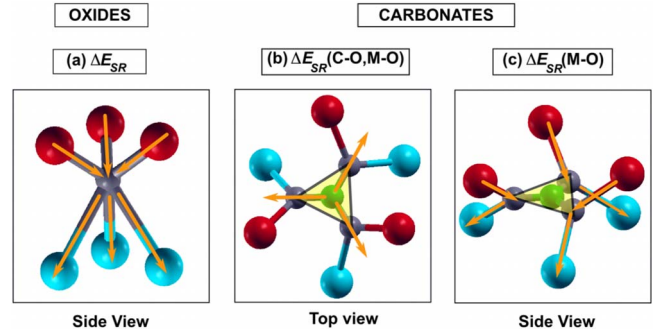

FIG. 3. (Color online) (a) M-O bond relaxation of the oxygen-centered octahedra of the $(CaO)_1/(MgO)_1$ (111) structure, (b) *internal* CO_3-centered relaxation of the $(CaCO_3)_1/(MgCO_3)_1$ (111) dolomite structure, and (c) *external* CO_3-centered relaxation of the $(CaCO_3)_1/(MgCO_3)_1$ (111) dolomite structure. The atoms are calcium (blue/gray spheres), magnesium (red/dark gray spheres), oxygen (small gray spheres), and carbon (small green/gray spheres), where the triangles highlight the planar carbonate groups.

relaxation step so has slightly higher ΔH compared with the ordered (111).

B. Carbonates

The ΔE_{SR} values are very negative (<−650 meV/cation pair) (Table I). In this case, the relaxation is not only due to the Ca-O and Mg-O bonds but the change in the CO_3 group is significant (Table IV). In order to better determine the contributions of the C-O and M-O relaxations in the ΔE_{SR} step, the positions of the oxygen atoms in S4 are allowed to relax while the cation and carbon positions are kept fixed, resulting in the intermediate (S4b) structure (Table IV). ΔE_{SR} can therefore be broken into two components: $\Delta E_{SR}(C-O,M-O)$ and $\Delta E_{SR}(M-O)$. The $E_{SR}(C-O,M-O)$ relaxation can be understood as an *internal* CO_3 group breathing-mode relaxation where the C-O bonds lengthen to their final length, maintaining the 120° O-C-O bond angles, as in Fig. 3(b). The M-O bond lengths adjust accordingly to this relaxation (physically, this involves the rotation of the cation-centered octahedra in the (111) plane). The

TABLE III. Bond lengths (Å) for CaO, MgO (S1), and the mixed phases before (S4) and after (S5) the structural relaxation step (ΔE_{SR}). Bond lengths in $\langle \; \rangle$ are averaged values.

Structure	Phase	d_{Ca-O}	d_{Mg-O}	ΔE_{SR}
S1	CaO(=Ideal)	2.420		
	MgO(=Ideal)		2.129	
S4	Ordered (001) $(\bar{V}; u_0)$	2.303	2.303	
	Ordered (111) $(\bar{V}; u_0)$	2.280	2.280	
	Random $(\bar{V}; u_0)$	2.289	2.289	
S5	Ordered (001)	2.303	2.303	−1
	Ordered (111)	2.354	2.210	−227
	Random	$\langle 2.298 \rangle$	$\langle 2.183 \rangle$	−199

TABLE IV. Bond lengths (Å) for $CaCO_3$, $MgCO_3$, (S1) and the mixed phases before (S4), intermediate (S4b) and after (S5) the structural relaxation step (ΔE_{SR}). Bond lengths in $\langle \rangle$ are averaged over values. O-C-O bond angles are all 120° (except for the S5 random structure, where they are on average 119.5°).

Structure	Phase	$d_{\text{Ca-O}}$	$d_{\text{Mg-O}}$	$d_{\text{C-O}}$	ΔE_{SR}	
S1	$CaCO_3$(=Ideal)	2.387		1.299		
	$MgCO_3$(=Ideal)		2.131	1.297		
S4	Ordered (111) $(\bar{V}; u_0)$	2.272	2.272	1.261		
	Random $(\bar{V}; u_0)$	2.277	2.277	1.264		
S4b	Ordered (111) $(\bar{V}; u_{\text{(C-O)}})$	2.377	2.152	1.298	−708	ΔE_{SR}(C-O,M-O)
	Random $(\bar{V}; u_{\text{(C-O)}})$	$\langle 2.263 \rangle$	$\langle 2.141 \rangle$	$\langle 1.298 \rangle$	−499	
S5	Ordered (111)	2.406	2.113	1.298	−178	ΔE_{SR}(M-O)
	Random	$\langle 2.315 \rangle$	$\langle 2.100 \rangle$	$\langle 1.298 \rangle$	−170	

ΔE_{SR}(M-O) relaxation is the *external* CO_3 group relaxation, where the CO_3 group is effectively a fixed object and moves closer to Mg and further from Ca atoms, Fig. 3(c), analogous to the oxygen asymmetric relaxation described for the ΔE_{SR} step for the oxides [Fig. 3(a)].

Here we find for the (111) ordered structure, ΔE_{SR}(C-O,M-O)=−708, ΔE_{SR}(M-O)=−178 meV/cation pair, and for the random structure, ΔE_{SR}(C-O,M-O)=−499, ΔE_{SR}(M-O)=−170 meV/cation pair. Clearly, ΔE_{SR}(C-O,M-O) is large and negative while the magnitude of ΔE_{SR}(M-O) is consistent with the ΔE_{SR} of the (111) ordered and random oxides, which also consists of only M-O relaxations (Table III). Thus, ΔE_{SR}(C-O,M-O) is the distinguishing feature between a single-atom common anion, (Ca,Mg)O, and a common anion *group*, (Ca,Mg)CO$_3$, and the cause of its stability over oxides. The results show that the ΔE_{SR} depends on two main factors: (i) *The internal CO_3 group relaxation*. Naturally, the strongest bonds in the structure will contribute significantly to the relaxation energy. Using bond length as an indication of bond strength, the strongest bonds in the carbonates are C-O > Mg-O > Ca-O. A significant proportion of the ΔE_{SR}(C-O,M-O) must be due to the C-O bond relaxation within the CO_3 group even if the change in bond length is small, 0.04 Å (from 1.26 to 1.30 Å, Table IV). This CO_3 group stiffness is in agreement with the strongest ordering interaction parameter being found across the CO_3 group.[40,41] (ii) *Approaching ideal bond geometry*. While the stiffness of the C-O bonds in the ordered (111) carbonate allow C-O to reach the ideal bond length (1.30 Å), the weaker M-O bonds are able to get close to ideality, where $\Delta d_{\text{Ca-O}}$(S5-ideal)=0.019 Å and $\Delta d_{\text{Mg-O}}$(S5-ideal)=−0.018 Å (Table IV). This is much closer to ideality than is achieved by the ordered (111) oxide, where $\Delta d_{\text{Ca-O}}$(S5-ideal)=−0.066 Å and $\Delta d_{\text{Mg-O}}$(S5-ideal) =0.081 Å (Table III). Assuming then that the stiff CO_3 can be treated as a rigid entity, this means that *the presence of CO_3 allows M-O to get closer to ideal positions in dolomite than can be achieved in the oxide*. In fact the total M-O relaxation distances in the ΔE_{SR} step [for both E_{SR}(C-O,M-O) and E_{SR}(M-O)] for the ordered (111) carbonate [$\Delta d_{\text{Ca-O}}$(S5-S4)=0.134 Å and $\Delta d_{\text{Mg-O}}$(S5-S4)=−0.159 Å] (Table IV) is much larger than for the ordered (111) oxide [$\Delta d_{\text{Ca-O}}$(S5-S4)=0.074 Å and $\Delta d_{\text{Mg-O}}$(S5-S4)=−0.070 Å] (Table III).

C. Comparing the ordered carbonate with the random carbonate

As was seen in Sec. V, the chemical exchange energy, ΔE_{CE}, is negative but small for the carbonates, showing that the *chemical effect* of cation arrangement is not in itself responsible for the negative enthalpy of the ordered carbonate and the large, positive value of the random carbonate. Interestingly though, defect calculations using a shell model,[25] and separately, cluster expansion calculations[37,39] found that the carbonate system favors intralayer clustering (e.g., Ca-Ca) and interlayer ordering (Ca-Mg), such that the layered dolomite structure is favored.

We find that in ordered (111) dolomite, the CO_3 groups remain planar and parallel to the (111) plane for all structures (S1-S5). The separation of Ca and Mg into pure Ca and pure Mg layers in ordered (111) dolomite allows the CO_3 groups to remain planar and therefore reach ideal bond lengths and angles. However, in the S5 relaxed structure of the random carbonate, the CO_3 groups are distorted, no longer with planar geometry, and slightly tilted out of the (111) plane by the random distribution of cations within each layer. Previous lattice-energy calculations have shown the importance of planarity for minimizing the formation enthalpy.[36] The average C-O bond lengths are still close to ideal (1.30 Å, Table IV) but the range in fact varies from 1.29–1.31 Å. Similarly the M-O bonds are away from ideality in the random carbonate, $\Delta d_{\text{Ca-O}}$(S5-ideal)=−0.072 Å and $\Delta d_{\text{Mg-O}}$(S5-ideal)=−0.031 Å, using the averaged values, which nevertheless show atoms further from ideality than the ordered carbonate. The structural disruption costs the random system 209 meV/cation pair more in the ΔE_{SR}(C-O,M-O) step compared to the ordered (111) dolomite (Table IV). The energy from internal relaxation is not enough to compensate the ΔE_{VD} and ΔE_{SD} steps, and random dolomite hence has a positive enthalpy.

VII. CONCLUSIONS

For isovalent, isostructural $A_xB_{1-x}X$ alloys, the main contributing factor to the formation enthalpy is the volume deformation, ΔE_{VD}, since all other terms are smaller. For alloys, where X is a *group*, ΔE_{VD} is still large, but structural relaxation becomes the most important term. The presence of the a stiff anion such as CO_3 allows more internal degrees of freedom for the A-X and B-X bonds to relax to ideal lengths. This provides an explanation for the low formation energy of $x_{Mg}=50\%$ ordered dolomite. However, distortion of the CO_3 group caused by random cation arrangement raises the formation enthalpy, which may be the reason why there are so few ground states [just ordered (111) dolomite] in the $CaCO_3$-$MgCO_3$ system.[39,41]

A larger, less rigid anion molecule, with more flexible bonds may be able to increase the dominance of the ΔE_{SR} term enough while allowing a greater range of structures at different compositions to exist. A smaller, more rigid, anion molecule would increase the effect of chemical exchange, ΔE_{CE}, but may make it more difficult for the overall structure to reach ideal bond lengths at the end of the ΔE_{SR} step.

Understanding the mechanism for the classic CaO, MgO, $CaCO_3$, and $MgCO_3$ systems could facilitate, in the future, ways of converting phase-separating alloys with undesirable microstructure, to more stable alloys with uniform microstructure, a central issue in electronic materials.

ACKNOWLEDGMENTS

*alex.zunger@nrel.gov

[1] G. Stringfellow, J. Cryst. Growth **27**, 21 (1974).

[2] A. Zunger and S. Mahajan, *Handbook of Semiconductors* (Elsevier Science B. V., Amsterdam, 1994), Vol. 3, p. 1399.

[3] M. B. Panish and M. Ilegems, in *Prog. Sol. State Chem*, edited by M. Reiss and J. O. McCaldin (Pergamom, New York, 1972), p. 39.

[4] L. M. Foster, J. E. Scardefield, and J. F. Woods, J. Electrochem. Soc. **119**, 765 (1972).

[5] A. B. Chen and A. Sher, *Semiconductor Alloys: Physics and Materials Engineering* (Plenum, New York, 1995).

[6] J. L. Martins and A. Zunger, J. Mater. Res. **1**, 523 (1986).

[7] R. G. Dandrea, J. E. Bernard, S.-H. Wei, and A. Zunger, Phys. Rev. Lett. **64**, 36 (1990).

[8] P. K. Davies and A. Navrotsky, J. Solid State Chem. **46**, 1 (1983).

[9] J. H. Burns and W. R. Busing, Inorg. Chem. **4**, 1510 (1965).

[10] H.-C. Gaebell, G. Meyer, and R. Hoppe, Mater. Res. Bull. **18**, 429 (1983).

[11] G. Spinolo and U. Anselmi-Tamburini, J. Phys. Chem. **93**, 6837 (1989).

[12] We will denote a random alloy of composition x as $A_xB_{1-x}X$ and an ordered (superstructure) as $(AX)_n/(BX)_m$.

[13] R. C. Doman, J. B. Barr, R. N. McNally, and A. M. Alper, J. Am. Ceram. Soc. **46**, 313 (1963).

[14] P. L. Althoff, Am. Mineral. **62**, 772 (1977).

[15] L. Chai, A. Navrotsky, and R. J. Reeder, Geochim. Cosmochim. Acta **59**, 939 (1995).

[16] A. Navrotsky and C. Capobianco, Am. Mineral. **72**, 782 (1987).

[17] A. Navrotsky, D. Dooley, R. Reeder, and P. Brady, Am. Mineral. **84**, 1622 (1999).

[18] M. Weil, Cryst. Res. Technol **42**, 1058 (2007).

[19] B. Matkovic, S. Popovic, B. Grzeta, R. Halle, J. Am. Ceram. Soc. **69**, 132 (1986).

[20] E. M. Aleksandrov, G. P. Kozlovskaya, and L. F. Piteva, Inorg. Mater. **12**, 1669 (1976).

[21] T. Takamori and J. J. Boland, J. Appl. Phys. **64**, 2130 (1988).

[22] P. D. Tepesch, A. F. Kohan, G. D. Garbulsky, G. Ceder, C. Coley, H. T. Stokes, L. L. Boyer, M. J. Mehl, B. P. Burton, K. Cho, and John Joannopoulos, J. Am. Ceram. Soc. **79**, 2033 (1996).

[23] A. F. Kohan and G. Ceder, Phys. Rev. B **54**, 805 (1996).

[24] C. R. A. Catlow and W. C. Mackrodt, in *Computer Simulation of Solids*, edited by C. R. A. Catlow and W. C. Mackrodt (Springer, Berlin, 1982).

[25] D. K. Fisler, J. D. Gale, and Randall T. Cygan, Am. Mineral. **85**, 217 (2000).

[26] V. L. Vinograd, M. H. F. Sluiter, and Björn Winkler, Phys. Rev. B **79**, 104201 (2009).

[27] D. C. Sayle, S. A. Maicaneanu, B. Slater, and C. R. A. Catlow, J. Mater. Chem. **9**, 2779 (1999).

[28] N. H. de Leeuw, Am. Mineral. **87**, 679 (2002).

[29] M. Y. Lavrentiev, N. L. Allan, G. D. Barrera, and J. A. Purton, J. Phys. Chem. B **105**, 3594 (2001).

[30] N. L. Allan, G. D. Barrera, M. Y. Lavrentiev, I. T. Todorov, and J. A. Purton, J. Mater. Chem. **11**, 63 (2001).

[31] M. Sanati, G. L. W. Hart, and A. Zunger, Phys. Rev. B **68**, 155210 (2003).

[32] S. V. Stolbov and R. E. Cohen, Phys. Rev. B **65**, 092203 (2002).

[33] C. E. Mohn, M. Y. Lavrentiev, N. L. Allan, E. Bakken, and S. Stølen, Phys. Chem. Chem. Phys. **7**, 1127 (2005).

[34] V. S. Urusov, T. G. Petrova, and N. N. Eremin, Crystallogr. Rep. **53**, 1030 (2008).

[35] V. S. Urusov, J. Solid State Chem. **153**, 357 (2000).

[36] P. A. Rock, G. K. Mandell, W. H. Casey, and E. M. Walling, Am. J. Sci. **301**, 103 (2001).

[37] B. P. Burton, Am. Mineral. **72**, 329 (1987).

[38] B. P. Burton and R. Kikuchi, Am. Mineral. **69**, 165 (1984).

[39] B. P. Burton and A. V. de Walle, Phys. Chem. Miner. **30**, 88 (2003).

[40] V. L. Vinograd, Björn Winkler, A. Putnis, J. D. Gale, and M. H. F. Sluiter, Chem. Geol. **225**, 304 (2006).

[41] V. L. Vinograd, B. P. Burton, J. D. Gale, N. L. Allan, and B. Winkler, Geochim. Cosmochim. Acta **71**, 974 (2007).

[42] G. P. Srivastava, J. L. Martins, and A. Zunger, Phys. Rev. B **31**, 2561 (1985).

[43] J. E. Bernard, L. G. Ferreira, S. H. Wei, and A. Zunger, Phys. Rev. B **38**, 6338 (1988).

[44] D. M. Wood, S.-H. Wei, and A. Zunger, Phys. Rev. B **37**, 1342 (1988).

[45] G. Kresse and J. Furthmüller, *VASP the Guide* (Universität Wien, Wien, Austria, 2007).

[46] Number of *k* points used: 666 for the 2-cation cell of the (111) oxide, 172 for the 4-cation cell of the (001) oxide, 63 for the 16-cation cell of the random oxide, 172 for the 4-cation cell of the (111) carbonate, and 20 for the 16-cation cell of the random carbonate.

[47] A. Zunger, S.-H. Wei, L. G. Ferreira, and J. E. Bernard, Phys. Rev. Lett. **65**, 353 (1990).

[48] Landolt-Bornstein: *Numerical Data and Functional Relationships in Science and Technology*, edited by K.-H. Hellwege and A. M. Hellwege, New Series, Group III, Vol. 7b1 (Springer-Verlag, Berlin, 1975).

[49] Z. Feng and M. S. Seehra, Phys. Rev. B **45**, 2184 (1992).

[50] J. Zhang and R. J. Reeder, Am. Mineral. **84**, 861 (1999).

[51] R. J. Reeder and Y. Nakajima, Phys. Chem. Miner. **8**, 29 (1982).

[52] The atomic charge is integrated within a radius of 1.3 Å for Ca and 1.1 Å for Mg.

[53] Here, "ideal" is defined as a structure whose structural parameters equal the values in the prototype compounds. For example, ideal CaMgO is a structure of the pseudobinary CaMgO where the Ca-O and Mg-O bond lengths equal the respective values on CaO and MgO, respectively.